PAPER

Check for updates

Boron isotopic analysis in bulk silicate materials using the Neoma MS/MS MC-ICP-MS

Sean R. Scott, [ID] * Matthew A. Coble, [ID] Natalie E. Sievers, Kirby P. Hobbs, [ID] Tyler D. Schlieder [ID] and Mindy M. Zimmer

Boron (B) isotopes are a valuable tracer with applications ranging from geological, environmental, and nuclear studies because B isotopic fractionation is highly sensitive to chemical processes yielding distinct isotopic trends in natural and anthropogenic systems. Despite this wide applicability, there remain relatively few measurements on well-described reference materials and in some cases, poor agreement between various methods. We report a method for boron isotope ratio measurement in solution on the Neoma MS/MS MC-ICP-MS specifically targeting bulk silicates. We evaluate the performance of the method and instrument as it relates to the measurement of the absolute boron isotope ratio ($^{10}B/^{11}B$). The results indicate that the method produces data in agreement with literature values and that the sample–standard bracketing technique is appropriate for the Neoma MS/MS MC-ICP-MS which has been in use for decades on previous generation instruments. Careful tuning of the MS/MS lenses is required to obtain precision comparable to non MS/MS equipped MC-ICP-MS. With careful tuning, internal and external precisions of $\sim 0.3\text{‰}$ were achieved. However, when the MS/MS is not properly tuned external precisions exceed 3‰. Nevertheless, our results for IAEA B-6, BCR-2, BHVO-2 and W-2a reference materials overlap the 1σ range of previously reported $^{10}B/^{11}B$. Data are reported for total boron quantities down to a few tens of nanograms. Our procedure yielded blanks as low as 3 ng but up to 29 ng, making blank corrections important for small samples sizes in the few 10s of nanogram range. We report B isotope ratios for AGV-2G, SL-1G, GSC-2G, GSD-2G, GSE-2G, RLS-132, RLS-140, NKT-1G, and T1-G glass reference materials that have not been previously reported in the literature.

1. Introduction

Variations in the natural isotopic composition of B were recognized in the early days of isotopic analysis by mass spectrometry.[1] Boron isotopes have since been used in various geological and environmental studies to track the causes and effects of natural and anthropogenic feedback mechanisms (see ref. 2 and 3). In these studies, B data are typically reported in delta notation ($\delta^{11}B$), which reports isotopic ratios of samples relative to a standard in units of permil (‰). The total variation in B isotopes in geological and environmental samples ranges from approximately -30 to $+60\text{‰}$.[4] In addition to investigations of natural phenomena, B is used in various forms in nuclear materials due to the high neutron capture cross-section properties of ^{10}B.[5,6] For these applications, delta notation has not been adopted in favor of the absolute isotope ratio because the B isotope composition varies by 10s of % in nuclear materials (*e.g.*, ref. 7).

Several methods are currently available for analysis of B isotopic composition, the most common being thermal ionization mass spectrometry (TIMS) and multi-collector inductively coupled plasma mass spectrometry (MC-ICP-MS) for bulk sample analysis.[8] Secondary ionization mass spectrometry (SIMS) and laser ablation MC-ICP-MS have also been used for *in situ* analyses (*e.g.*, ref. 9–12). The lowest possible uncertainty of the $^{10}B/^{11}B$ by any method corresponds to the uncertainty of the primary B isotopic standard (NIST951), which has a certified B isotopic composition of $^{10}B/^{11}B = 0.2473 \pm 0.0002$ (an uncertainty of 0.08% or 0.8‰).[13] This uncertainty is slightly higher than the uncertainties in delta notation that have been achieved in interlaboratory studies using modern mass spectrometry techniques ($\leq 0.6\text{‰}$).[14] Therefore, the propagated uncertainty for the absolute isotopic composition of B is larger than what can be achieved by measuring one material relative to another (*i.e.*, delta notation). For nuclear applications, the uncertainty in the absolute $^{10}B/^{11}B$ is the more relevant metric, rather than the reproducibility of delta values.

Bulk sample analysis of B isotopes is challenging because B is particularly volatile during hydrofluoric acid digestions due to the formation of volatile BF_3. In addition, B is susceptible to laboratory contamination due to the relative difficulty of controlling B procedural blanks.[15] Several methods for dissolution and B purification have been used depending on the

Pacific Northwest National Laboratory, 902 Battelle Blvd, Richland, WA 99354, USA. E-mail: sean.scott@pnnl.gov

sample type being investigated,[16–18] especially for silicates that often require complex sample treatments for accurate isotopic analysis due to volatilization of B that can fractionate the isotopic composition. Ishikawa and Nakamura[19] determined that B volatilization from hydrofluoric acid could be suppressed using a B-mannitol complex, and this method has been adopted for B concentration and isotopic analysis in silicate materials that undergo acid digestions (e.g., ref. 20–23). Once retained in solution, B has been purified using a combination of anion and cation exchange resins to remove impurities that could impart matrix effects during isotopic analysis and lead to inaccuracies in isotopic composition.[16,17,20,24,25]

The volatility of B in the absence of mannitol has also been exploited using microsublimation techniques.[18,24,26] Under proper conditions, microsublimation techniques provide a mechanism for B purification that does not require additional ion exchange procedures, thus reducing the potential for contamination. Alternatively, B has also been measured by fusing silicate samples with a low-B KCO_3 flux.[25,27] The melted pellet is then dissolved in water, keeping the solution neutral and allowing for purification using B specific ion exchange resins (e.g., Amberlite IRA-473). Most importantly, to avoid fractionation, a representative analysis of a bulk sample requires that boron should be completely recovered from the sample matrix without contamination from external sources, both of which can lead to spurious results during mass spectrometry measurements.[19,20]

In this study, we present a method for boron isotope analysis of bulk silicate materials in solution on the Neoma MS/MS MC-ICP-MS. An approach involving the mannitol–HF digestion was adopted, employing both cation and anion exchange resins to purify B for accurate isotopic analysis. The performance of the mass spectrometer was evaluated for measurement of $^{10}B/^{11}B$ with reported uncertainties that include the overall uncertainty in the absolute boron isotopic composition of natural boron represented by the NIST951 boric acid isotopic standard. 10^{13} Ohm resistors were used for the isotopic analysis that allowed precise isotopic measurements of total boron quantities in the single digit nanogram range. $^{10}B/^{11}B$ data are presented, along with associated uncertainties for several reference materials with well characterized boron isotopic compositions based on published $\delta^{11}B$ values, as well as reference materials for which boron isotopes have not been previously reported. These data show that $^{10}B/^{11}B$ can be measured on the Neoma MS/MS MC-ICP-MS with similar accuracy and precisions to previous generation results by MC-ICP-MS and TIMS. However, careful tuning of the MS/MS lenses is required.

2. Experimental

All chemical and analytical procedures were carried out at the physical sciences facilities at the Pacific Northwest National Laboratory campus in Richland, Washington, USA. Wet chemical procedures were conducted in the ultra-trace isotopic and elemental analysis facility, and the samples were transferred to the Materials Testing and Production Laboratory that houses the Neoma MS/MS MC-ICP-MS for isotopic analysis. The Neoma

MS/MS is an MC-ICP-MS equipped with a double-Wien filter and collision cell that provides improved abundance sensitivity, mass filtering capabilities, and ion separation capabilities using gas reactivities. Details on the design of this instrument are provided in ref. 28.

2.1 Sample digestion

Acid digestion of silicates for boron analysis requires relatively low temperatures and the use of a boron complexing agent to prevent volatilization. Our approach was similar to methods outlined in ref. 20 and 22. Up to 100 mg of silicate rock powder or small (<1 mm) glass chips were weighed into a PFA vial. The powder was soaked in a mannitol solution (0.1 or 1%) to provide a molar ratio of mannitol/boron > 1.[19] Then 0.1 ml of 30% H_2O_2 and 1 ml of 29 M HF were added (addition of the HF to silicate powder causes effervescence), and the vial was sealed and left on a hotplate at 70 °C for up to 3 days. The vial was removed from the hotplate and allowed to cool to room temperature. The solution containing residual fluorides was centrifuged and the supernatant (containing boron) was decanted into a PFA vial. The residual fluorides were rinsed with an additional 0.5 ml of 29 M HF, centrifuged, and decanted into the same sample vial. The 0.5 ml 29 M HF rinse was repeated. The solution was then dried at 70 °C, dissolved in 0.5 ml of 6 M HCl, and evaporated again. 1 ml of 0.1 M HCl was added to the final sample, capped, and heated briefly at 70 °C to dissolve.

In addition to the silicate samples, aliquots of seawater were also processed in a similar fashion to provide additional validation of the method and controls on isotopic composition. One gallon of offshore seawater was purchased from Carolina Biological Supply. This seawater is not a certified isotopic standard but is useful as a representative seawater sample that should possess the nominal isotopic compositions of various elements with long seawater residence times (e.g., Sr, Ca, Li, B, and U). One mL seawater samples were aliquoted into PFA vials, 200 μL of 0.1% mannitol was added, and the solutions were dried at 70 °C. The samples were then dissolved in 0.5 ml of 6 M HCl and evaporated again. 1 ml of 0.1 M HCl was added to the final sample, capped, and heated briefly at 70 °C to dissolve.

2.2 Purification of boron

Purification of B was achieved using a two-column procedure that included a cation exchange column followed by an anion exchange column.[20] The cation exchange column was calibrated using a NIST SRM2780a digestion solution in HCl that was doped with additional boric acid. 1.5 ml of Biorad AGMP50 (macroporous cation exchange resin) was used in a homemade "macro" column made from a disposable pipette tip. The reservoir of a 3 mL volumetric pipette tip was sliced off at the top, and a 4 mm diameter frit cut from a 1/16″ thick PTFE sheet using a circular cutting tool was inserted into the base of the column. Excess pipette material was sliced off the bottom. The resin was slurried in H_2O and pipetted into the column up to a line demarking 1.5 ml that had been measured by pipetting 1.5 ml of H_2O into the column. After settling, the resin was pre-cleaned with repeated 6 M HCl rinses and conditioned with

514 | J. Anal. At. Spectrom., 2026, 41, 513–525

This journal is © The Royal Society of Chemistry 2026

Boron elution AGMP50
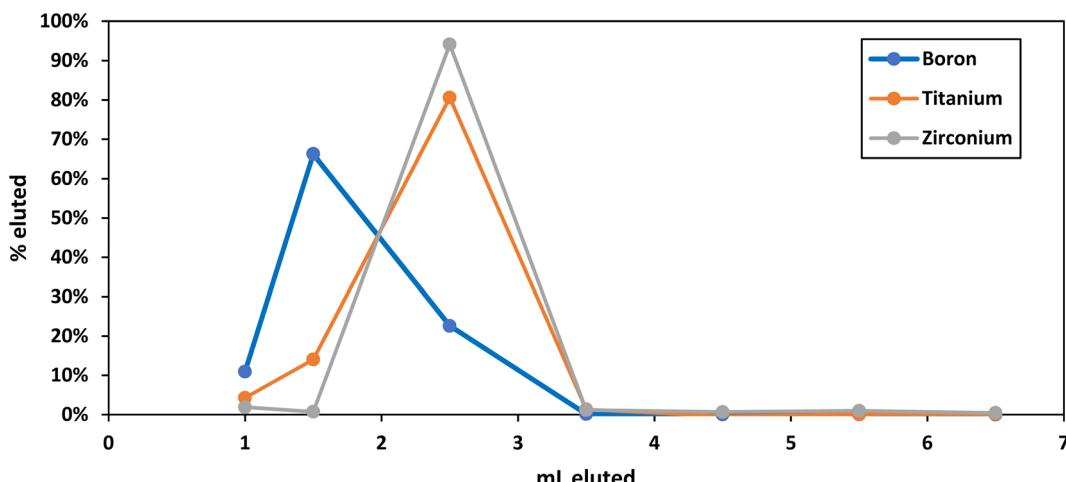
Fig. 1 Elution curve of boron on the AGMP50 cation exchange column. Titanium and zirconium are also shown for reference.

0.02 M HF. The sample was loaded in 0.1 M HCl, washed once with 0.5 ml of 0.02 M HF followed by multiple 1 ml washes of 0.02 M HF which were collected in separate PFA vials to determine the boron elution on a Thermo iCAP TQ ICPMS. This procedure is effective at removing major element cations (*e.g.*, iron and calcium[20]) that could cause isobaric interferences and/ or suppress the boron signal during analysis by mass spectrometry.

Elements such as titanium and zirconium elute with the boron during the cation exchange procedure (Fig. 1) and need to be separated using an anion column to produce a purified boron solution. The anion exchange column was calibrated using boric acid solution that was doped with mannitol, dried, then redissolved in 0.6 ml of 3M HF. The mannitol was added to simulate the sample matrix. Next, 0.3 ml of Biorad AG1-X4 100–200 mesh anion exchange resin was used in a homemade

"micro" column made from a disposable pipette tip. The reservoir of a 3 mL volumetric pipette tip was sliced off at the base of the reservoir, and a 1.5 mm diameter frit cut from a 1/16″ thick PTFE sheet using a circular cutting tool was inserted into the base of the column. The resin was slurried in H_2O and pipetted into the column up to a line demarking 0.3 ml that had been measured by pipetting 0.3 ml of H_2O into the column. After settling, the resin was pre-cleaned with washes of 6 M HCl and then conditioned with 0.02 M HF. The sample was loaded in 3 M HF, and then one 0.25 ml wash of 2 M HCl + 0.5 M HF followed by 0.3 ml washes of 2 M HCl + 0.5 M HF and 0.4 ml washes of 6 M HCl were collected in separate PFA vials to determine the boron elution on a Thermo iCAP ICPMS. The boron sticks to the anion resin in the presence of HF (while the remaining elements elute) and then elutes in 6 M HCl (Fig. 2). In the final procedure, 200 μl of 0.1% mannitol are added to the

Boron elution AG1-X4
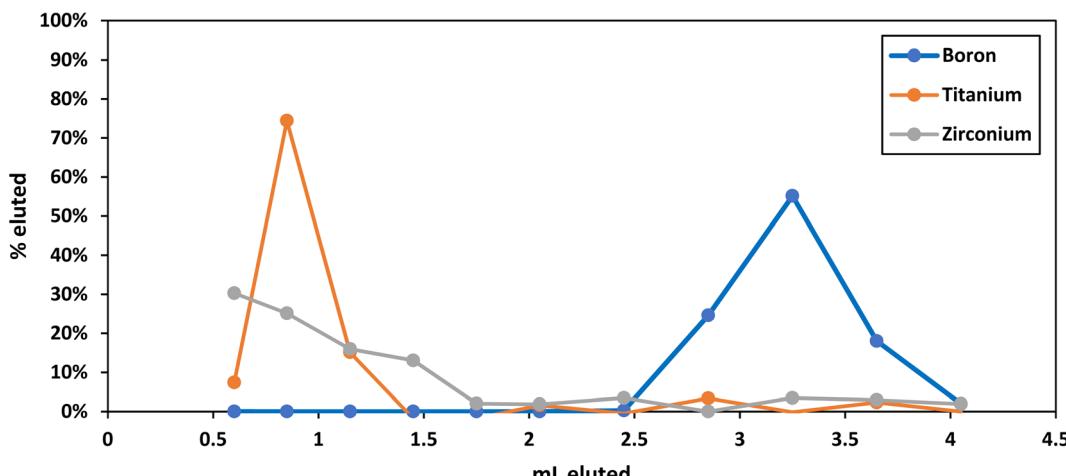
Fig. 2 Elution curve of boron on the AG1-X4 anion exchange column. Titanium and zirconium are shown for reference.

Table 1 Procedure for boron isotope analysis in bulk powders

Step	Reagent	Volume	Purpose	Action
AGMP50 1.5 ml	6 M HCl	10 ml	Clean	
	0.02 M HF	2 ml	Condition	
	0.1 M HCl	1 ml	Load sample	Collect B
	0.02 M HF	0.5 ml	Wash vial	Collect B
	0.02 M HF	3 ml	Elute B	Collect B
AG1-X4 100–200 0.3 ml	6 M HCl	4 ml	Clean	
	0.02 M HF	0.3 ml	Condition	
	3 M HF	0.6 ml	Load sample	
	2 M HCl + 0.5 M HF	0.25 ml	Wash vial	
	2 M HCl + 0.5 M HF	1.2 ml	Elute matrix	
	6 M HCl	2 ml	Elute B	Collect B

collection vial prior to beginning the boron collection to prevent volatilization. The calibrated ion exchange chromatography procedure is provided in Table 1.

2.3 Isotopic analysis of boron

Boron isotopes were measured on the Neoma MS/MS MC-ICP-MS. For routine analysis, the magnetic field of the double Wien mass filter component was set at ∼5% to minimize spread of the relatively low mass ion beams, and the electric field and other lenses were tuned to maximize sensitivity while minimizing instrument mass fractionation. As a result, the measured isotope ratios were consistent with typical mass bias values measure on MC-ICP-MS instruments without the double Wien mass filter (∼15% per amu). The lenses of the MS/MS were tuned to provide a "plateau" of isotopic ratio stability. This was achieved by scanning the electric field of the MS/MS while monitoring both the beam intensity of ^{11}B and the ^{10}B/^{11}B

isotopic composition. Increasing magnetic field settings were systematically evaluated for ion filtering capabilities in the low mass range, specifically focusing on Li–Be–B isotopes. ^{10}B and ^{11}B isotopes were measured on the L3 and H3 cups, respectively, and the quadruply charged ^{40}Ar beam was fully resolved from the ^{10}B peak (Fig. 3).

Table 2 Reproducibility metrics from individual analytical sessions

| Session	Solution	^{10}B/^{11}B	SD	RSD @ 2σ (‰)	n
1	GFS Boron	0.24722	0.00017	1.36	8
2	IV B	0.24740	0.00016	1.28	5
3	IV B	0.24736	0.00004	0.31	7
4	IV B	0.24713	0.00040	3.26	7
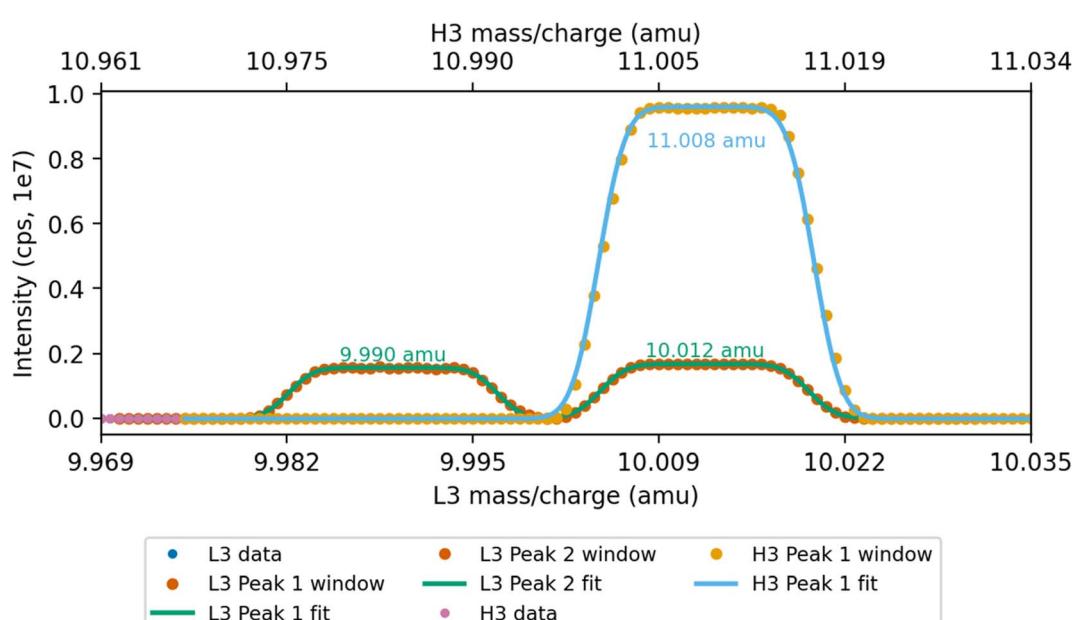
Fig. 3 Mass scan showing alignment of ^{10}B and ^{11}B on the L3 and H3 cups, respectively. The ^{40}Ar^{++++} beam is fully resolved from ^{10}B. The mass of this potential interference was confirmed using a slit-smeared Gaussian function. The slit-smeared Gaussian function is the same phenomenon as the "flat-topped" Gaussian described in ref. 42. Centroid masses of the ^{10}B and ^{11}B peaks are calculated based on the calibrated mass for each cup and are within 0.001 amu of the known masses.

Purified boron solutions were dried at 70 °C and then redissolved in 1 ml of 2% HNO_3 for isotopic analysis. All samples and standards were diluted to provide 10 ppb boron. In some cases, samples were diluted to no more than 2 ml when total boron was limited (e.g., BIR-1a). Samples were introduced into the plasma using the standard dual-pass cyclonic spray chamber, and the standard nickel sampler cone and X-series skimmer cone. Sensitivities up to 1.4×10^6 cps ^{11}B per ppb ($\sim$22 V ppm^{-1}) were achieved. To account for the elevated on-peak blanks due to boron memory effects in the spray chamber, a 15 minute washout was performed after each sample analysis, followed by an on-peak baseline measurement, which was subtracted from the next sample or standard analysis. Electronic baselines were measured before every blank, sample, and standard analysis using the default procedure in Qtegra software (60 1-second integrations). Boron isotopic compositions of samples were measured by sample–standard bracketing using a pure boric acid solution that was made using crystalline boric acid purchased from GFS Chemicals (Powell, Ohio, USA) and prepared gravimetrically. To correct for mass fractionation, the measured $^{10}B/^{11}B$ for each sample analysis was divided by the average of the standard measured before and after each sample and then multiplied by the assumed $^{10}B/^{11}B$ of 0.2473. Each analysis consisted of 30 4-second integrations measured on Faraday cups (L3 and H3) equipped with 10^{13} Ohm resistor amplifiers which enabled precise measurements of

relatively small boron beam currents (e.g., 29). Internal precisions were typically <0.30‰ (2SE). External precisions varied between sessions and samples, likely depending on the tuning of the double Wien filter (discussed below). Metrics for this external reproducibility based on pure boron solutions over four sessions are provided in Table 2. For purified samples, each individually purified aliquot was measured at least three times. Total boron quantities of the blanks and purified materials were estimated by comparing the beam intensities of the diluted solutions to the beam intensity of the GFS Chemicals primary standard. Blank corrections were completed by converting the total quantities of B to total atoms of each B isotope, then subtracting the number of atoms of each isotope in the blank from the number of atoms of each isotope in the sample and recalculating the isotopic ratio.

3. Results

3.1 Recoveries and blanks

Recovery metrics (total B recovered for each sample processed) are provided in Table 3. Several materials analyzed in this study did not have previously known B concentrations. New boron concentrations measured by SIMS at PNNL are also provided in Table 3. For samples with well known concentrations, B recoveries using the chemical procedures outlined here were highest for seawater (93.2 to 102%), whereas rock reference materials

Table 3 Boron recovery metrics for reference materials

Sample	Session/aliquot	B conc. ($\mu g\ g^{-1}$)	Aliquot (g)	B μg (exp.)	B μg (meas.)	Recovery (%)	Blank %
Seawater	1/1	4	1	4	3.7	93.2	0.79
	2/2	4	1	4	3.7	93.2	0.09
	3/3	4	1	4	4.1	102	0.30
IAEA B-6	1/1	203.8	0.01296	2.6	2.1	78.5	1.4
	2/2	203.8	0.02590	5.3	4.5	85.0	0.08
	3/3	203.8	0.02233	4.6	3.8	82.9	0.33
BCR-2	1/1	4.4	0.09130	0.40	0.36	88.5	8.3
	2/2	4.4	0.09570	0.42	0.32	77.1	1.1
BHVO-2	1/1	2.95	0.09733	0.29	0.24	82.0	13
	2/2	2.95	0.09160	0.27	0.18	65.8	2.0
BIR-1a	1/1	0.25	0.09695	0.024	0.045	185	65
	2/2	0.25	0.12090	0.030	0.017	55.3	21
	4/3	0.25	0.08649	0.022	0.018	84.6	52
W-2a	1/1	11.7	0.08033	0.94	0.88	93.5	3.4
	1/2	11.7	0.09910	1.2	1.07	91.9	2.8
	2/3	11.7	0.09910	1.2	0.88	75.5	0.40
GSC-2G	4/1	9.5[a]	0.06669	0.63	0.30	47.7	3.1
GSD-2G	4/1	53.4[a]	0.03767	2.0	0.65	32.4	1.5
GSE-2G	3/1	473[a]	0.04383	21	16	77.0	0.08
	4/2	473[a]	0.02111	9.9	8.4	83.8	0.11
NKT-1G	4/1	10.2[a]	0.01646	0.17	0.15	91.4	6.2
RGM-2	2/1	27.4	0.05090	1.4	1.3	91.6	0.27
RLS 140	3/1	51.2[a]	0.03177	1.6	1.5	89.8	0.70
RLS-132	4/1	16.8[a]	0.01317	0.22	0.21	94.1	4.5
SL-1G	3/1	54.2[a]	0.07232	3.9	4.4	113.2	0.28
T1-G	4/1	4[a]	0.01044	0.042	0.040	94.9	24
TB-Macusani	3/1	1756[a]	0.02904	51	47	92.3	0.03
AGV-2G	3/1	9.3[a]	0.09559	0.89	1.8	197	0.70

[a] Measured by SIMS at PNNL.

Table 4 Blank amounts and compositions

Session	Blank (µg)	$^{10}B/^{11}B$	Uncertainty ±
1	0.029	0.24485	0.00022
2	0.0035	0.24418	0.00028
3	0.012	0.24524	0.00033
4	0.0094	0.24630	0.00095

ranged from 65 to 92% except for BIR-1a that showed significantly more variable recoveries (55 to 185%). The >100% recovery for one BIR-1a analysis is likely due to the blank contribution from that batch of samples. Samples with new PNNL SIMS values showed recoveries mostly within that range, albeit with some exceedances. GSC-2G and GSD-2G gave low recoveries of 47 and 32%, whereas SL-1G and AGV-2G gave high recoveries of 113 and 197%. Potential heterogeneity within these samples is unknown.

The total quantities and isotopic compositions of procedural blanks are provided in Table 4. The procedural blank associated with the measured values from session 1 in Table 3 was elevated (29 ng) relative to the expected values that were obtained during the method development (3 ng). The blank associated with samples in session 2 was 3.5 ng, 12 ng in session 3, and 9.4 ng in session 4. Uncertainties in the blank contents range from 0.2 to

3.5% based on the standard deviations of repeat measurements. The isotopic compositions of the blank ranged from $^{10}B/^{11}B =$ 0.2442 to 0.2463. Table 3 also provides the blank percentage for each sample, which is calculated by dividing the blank from each respective batch by the total B recovered for each sample.

BIR-1a contains the lowest estimated B concentration of any material measured in this study. The estimated BIR-1a B concentration is based on the value reported for BIR-1 in ref. 30 of 0.25 ppm. Reference values for BIR-1 and BIR-1a range from 0.165 to 1.515 ppm from values compiled in the GEOREM database. Using the blank corrected B quantity recovered, the concentration of B in BIR-1a is 0.07 to 0.16 ppm. This is at least an order of magnitude lower in B content than any other material analyzed in this study, and thus highly sensitive to B contamination from procedural blanks.

3.2 Boron isotopic compositions

Boron isotope ratios ($^{10}B/^{11}B$) of seawater and rock reference materials are provided in Table 5. All uncertainties quoted are based on full error propagation using the Guide to the Expression of Uncertainty in Measurement (GUM) at a coverage factor of $k = 2$. This includes the uncertainty reported for the NIST 951a boric acid certificate of analysis and the standard deviations of multiple measurements of individual purified aliquots

Table 5 $^{10}B/^{11}B$ results for reference materials

Sample	Session/aliquot	n	$^{10}B/^{11}B_{meas.}$	Uncertainty ± ($k = 2$)	$^{10}B/^{11}B_{corr.}$ [a]	Uncertainty ± ($k = 2$)	Δ [b]	Literature [c]
Seawater	1/1	9	0.23808	0.00040	0.23802	0.00046	−0.023%	0.2379 ± 0.0002 [d]
	2/2	3	0.23850	0.00020	0.23850	0.00034	−0.002%	
	3/3	6	0.23801	0.00035	0.23799	0.00047	−0.009%	
IAEA B-6	1/1	6	0.24783	0.00034	0.24787	0.00041	0.017%	0.2474–0.2484
	2/2	3	0.24799	0.00022	0.24799	0.00036	0.001%	
	3/3	3	0.24806	0.00027	0.24807	0.00042	0.004%	
BCR-2	1/1	6	0.24862	0.00033	0.24896	0.00041	0.137%	0.2484–0.2488
	2/2	3	0.24888	0.00036	0.24893	0.00046	0.021%	
BHVO-2	1/1	6	0.24769	0.00025	0.24809	0.00033	0.164%	0.2474–0.2481
	2/2	3	0.24814	0.00023	0.24822	0.00037	0.032%	
BIR-1a	1/1	7	0.24573	0.00025	0.24739	0.00034	0.676%	0.2476 ± 0.0003 [e]
	2/2	3	0.24643	0.00049	0.24703	0.00057	0.241%	0.2486 ± 0.0002 [f]
	4/3	3	0.24632	0.00065	0.24856	0.00073	0.909%	
W-2a	1/1	6	0.24440	0.00025	0.24439	0.00033	−0.006%	0.2443–0.2458
	1/2	3	0.24436	0.00022	0.24434	0.00035	−0.006%	
	2/3	3	0.24507	0.00022	0.24507	0.00035	0.001%	
GSC-2G	4/1	3	0.24609	0.00020	0.24613	0.00038	0.015%	n/a
GSD-2G	4/1	6	0.24684	0.00068	0.24687	0.00075	0.012%	n/a
GSE-2G	3/1	3	0.24701	0.00028	0.24701	0.00043	0.001%	n/a
	4/2	3	0.24689	0.00035	0.24690	0.00048	0.001%	
NKT-1G	4/1	3	0.24215	0.00030	0.24189	0.00044	−0.111%	n/a
RGM-2	2/1	3	0.24883	0.00024	0.24885	0.00037	0.005%	n/a
RLS 140	3/1	6	0.24777	0.00036	0.24779	0.00049	0.009%	n/a
RLS-132	4/1	3	0.24879	0.00026	0.24901	0.00042	0.090%	n/a
SL-1G	3/1	3	0.24724	0.00020	0.24725	0.00039	0.002%	n/a
T1-G	4/1	3	0.24841	0.00062	0.24984	0.00071	0.576%	n/a
TB-Macusani	3/1	3	0.24972	0.00029	0.24972	0.00044	0.000%	n/a
AGV-2G	3/3	6	0.24947	0.00027	0.24950	0.00043	0.012%	0.2485 ± 0.0002 [g]

[a] Blank corrected $^{10}B/^{11}B$. [b] Difference in percent between blank corrected and measured $^{10}B/^{11}B$. [c] Literature data are MC-ICP-MS, P-TIMS, and LA-MC-ICP-MS data from the GeoREM database; uncertainties are 2SD. [d] Foster *et al.*, 2010.[31] [e] MC-ICP-MS data for BIR-1G.[32] [f] LA-MC-ICP-MS data for BIR-1 powder.[41] [g] MC-ICP-MS data for AGV-2.[24]

518 | *J. Anal. At. Spectrom.*, 2026, **41**, 513–525

This journal is © The Royal Society of Chemistry 2026

of the reference materials. The $^{10}B/^{11}B$ of each material agrees well with available literature values when $\delta^{11}B$ values are used to calculate the associated $^{10}B/^{11}B$. The measured $^{10}B/^{11}B$ of three seawater aliquots was 0.2381 ± 0.0004 ($n = 9$), 0.2385 ± 0.0002 ($n = 3$), and 0.2380 ± 0.0004 ($n = 6$), in good agreement with the canonical value reported in ref. 31 of 0.2379 ± 0.0002 (this value includes the propagated uncertainty from the primary NIST 951 reference standard). The $^{10}B/^{11}B$ values of USGS reference materials IAEA B-6, BCR-2, BHVO-2, and W-2a are all within the range reported in the literature (Fig. 5).
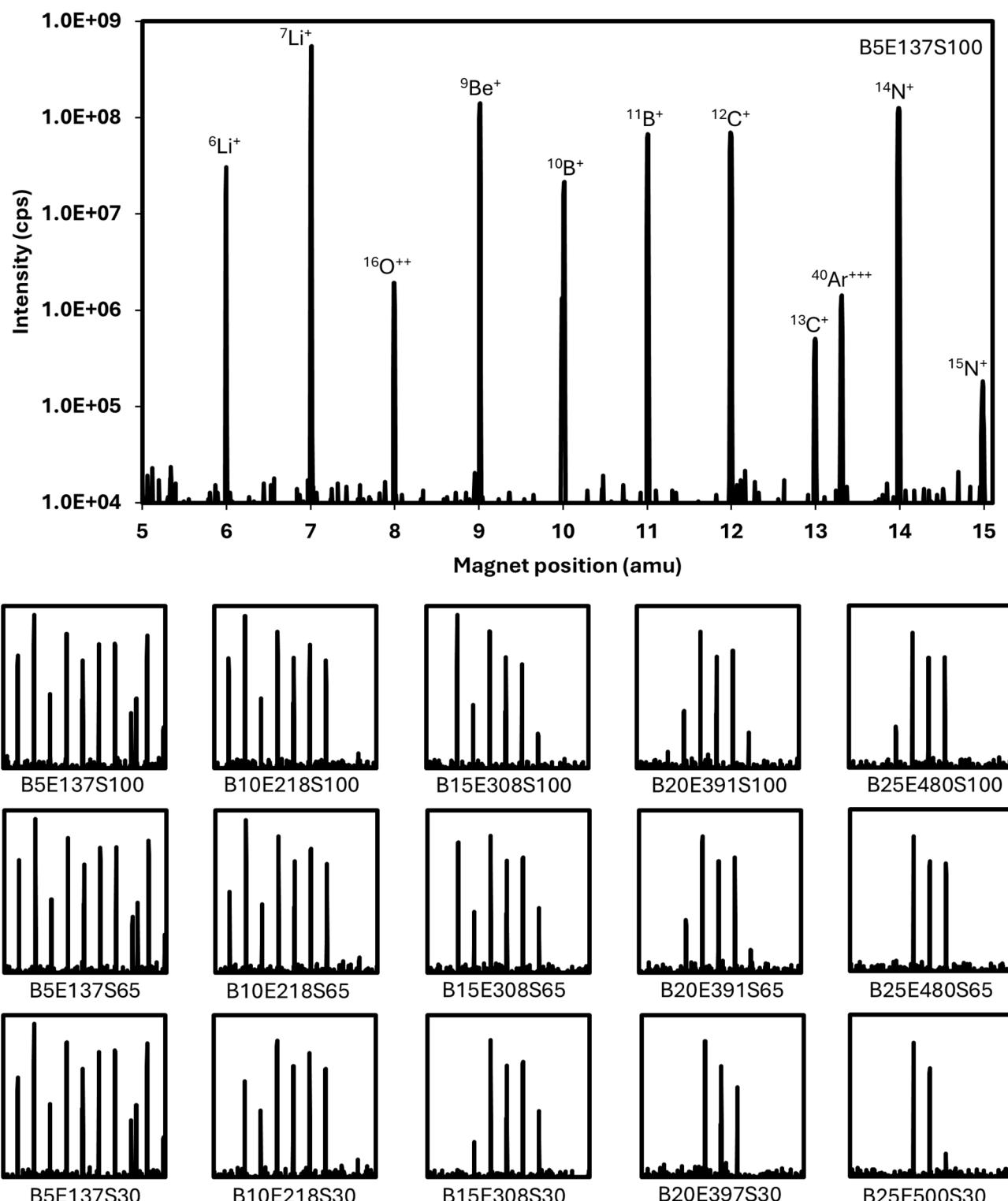
Fig. 4 Mass scans from 5–15 amu showing the transmission window for the light elements. The magnetic field (*B*), electric field (*E*), and slight width (*S*) are indicated as $B_{xx}E_{yy}S_{zz}$.

This journal is © The Royal Society of Chemistry 2026

J. Anal. At. Spectrom., 2026, **41**, 513–525 | **519**
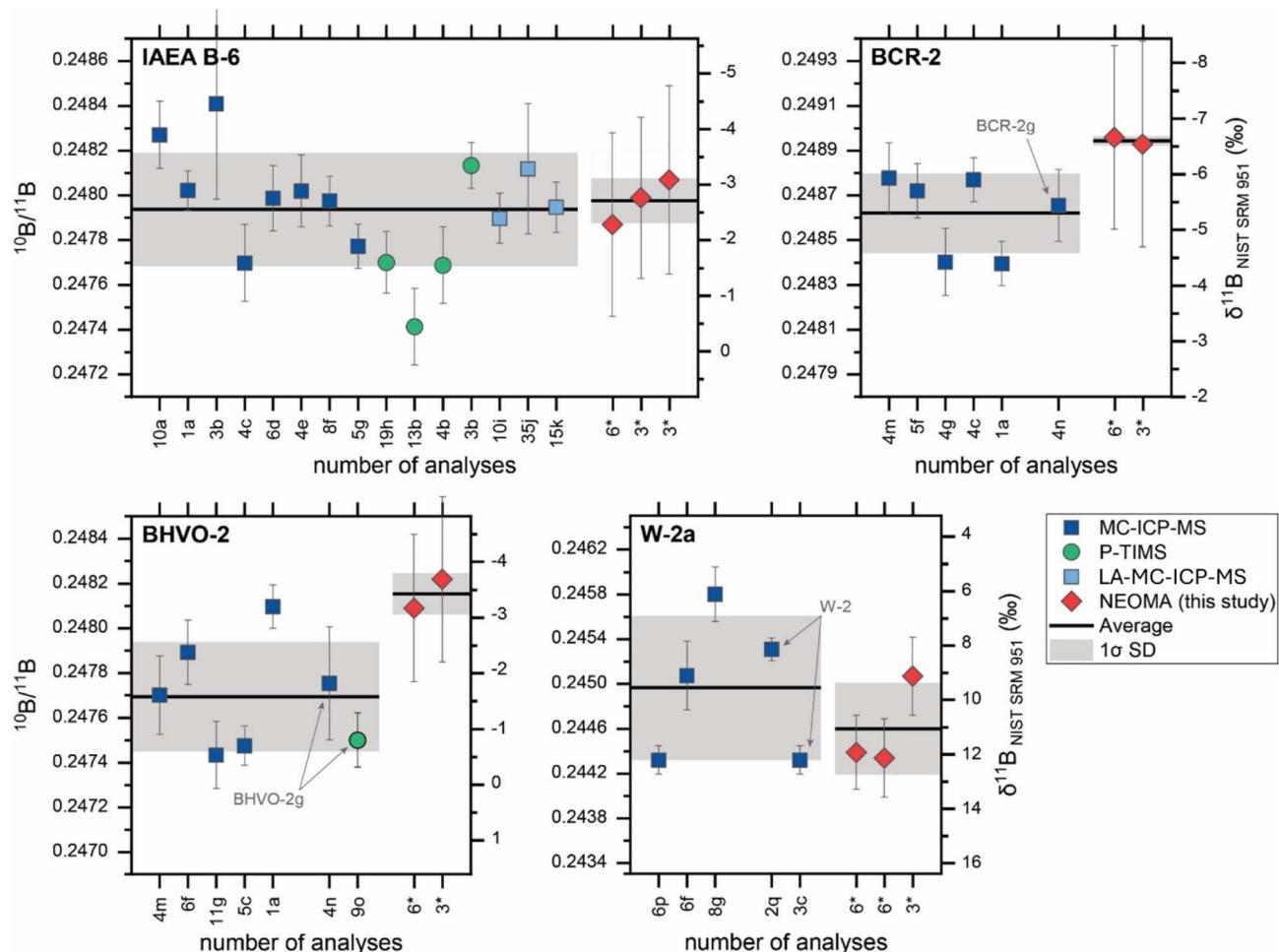
Fig. 5 Boron isotope composition reported as $^{10}B/^{11}B$ and in permil (‰, relative to NIST 951) for reference materials IAEA B-6, BCR-2, BHVO-2, and W-2a, comparing previously reported results measured by MC-ICP-MS, P-TIMS, and LA-MC-ICP-MS and new results measured by Neoma MS/MS MC-ICP-MS (this study). Note that most standards are measured as powders, but BCR-2g and BHVO-2g, measured as glass chips, are within the same range of powder measurements. Standards W-2 and W-2a were collected from the same location and represent different bulk aliquots of the same material. Individual error bars are shown at 1SD. Note that the vertical axis for W-2a is scaled at 0.5× relative to other plots, and the average and 1σ SD (thick black line and light grey box, respectively) for W-2a do not include data from reference g (see below). The horizontal axis denotes the number of analyses included in the reported mean value and the associated reference: a: ref. 18, b: ref. 35, c: ref. 22, d: ref. 23, e: ref. 36, f: ref. 37, g: ref. 38, h: ref. 39, i: ref. 40, j: ref. 9, k: ref. 41, m: ref. 43, n: ref. 32, o: ref. 44, p: ref. 45, q: ref. 24, and *: this study.

Several reference materials analyzed as powder in this study have no published $^{10}B/^{11}B$ data available for the powder, but $^{10}B/^{11}B$ data for the glass material are available (and *vice versa*). For example, BIR-1a analyzed in this study yielded a range of $^{10}B/^{11}B$ that overlaps the value reported for the glass BIR-1G after blank correction[32] at 1SD (Table 5). In contrast, the measured $^{10}B/^{11}B$ in this study for AGV-2G (glass) was 0.2495 ± 0.0003 and it does not overlap the published values for the power of 0.2485 ± 0.0002.[24] It is possible that the B isotopic composition of the powders has been fractionated or contaminated when powdered, despite both the glass and powder originating from the same stock of material. Notable, BCR-2 and BCR-2g, as well as BHVO-2 and BHVO-2g yielded values that overlap at 1 sigma (Fig. 5). The boron isotopic composition ($^{10}B/^{11}B$) of GSC-2G, GSD-2G, GSE-2G, NKT-1G, RLS 140, RLS-132, SL-1G, T1-G, and AGV-2G (Table 5) have not been previously reported in the literature.

Table 5 also provides the blank corrected $^{10}B/^{11}B$ based on the B contents recovered and blank levels of each respective batch of samples. Deviations between the blank corrected and measured isotopic ratios (Δ in Table 5) are mostly less than the minimum uncertainty of 0.08% with some exceptions. BIR-1a shows the largest deviations. Other significantly impacted samples include RLS-132, T1-G, and NKT-1G. The first aliquots of BCR-2 and BHVO-2 also showed deviations larger than the 0.08% minimum uncertainty. Blank corrections of the BCR-2 and BHVO-2 aliquots provide better agreement between duplicates than uncorrected values. Blank corrections for the three BIR-1a aliquots provide worse reproducibility, but overall better agreement with expected values from the literature.

3.3 Mass filtering capabilities of the MS/MS at low amu

The mass filtering capabilities for the light elements with the MS/MS can be adjusted to reach nearly 2 amu bandpass when

centered around ^{9}Be (Fig. 4). The B field that maintains maximum transmission of ^{9}Be was determined at ~25% of the maximum B field, where the E field was approximately 480V. At these high B/E fields, the adjustable slit between the two Wien filters of the MS/MS also provides some mass filtering capabilities which are more pronounced as the B field increases. For example, when the B field is 25%, decreasing the slit width from 100% to 65% eliminates the $^{16}O^{++}$ peak (Fig. 4). Further decreasing the slit width to 30% almost completely eliminates the ^{11}B peak (Fig. 4). For boron isotopic analysis no significant difference in peak shapes, potential interferences (e.g., quadruply charged ^{40}Ar), sensitivity, or isotopic ratio stability was observed as the B/E fields were increased. Thus, in this work

the B field was maintained at the 5% value to minimize mass dispersion through the MS/MS. However, the mass filtering capabilities at the low mass range may have other applications that were not explored during this study.

4. Discussion

4.1 Performance of the Neoma MS/MS for solution boron isotopic analysis

The performance of the Neoma MS/MS was evaluated over the course of multiple sessions comprising at least one analytical sequence each. Fig. 6 shows the raw $^{10}B/^{11}B$ of the primary boron standard measured throughout the first and second
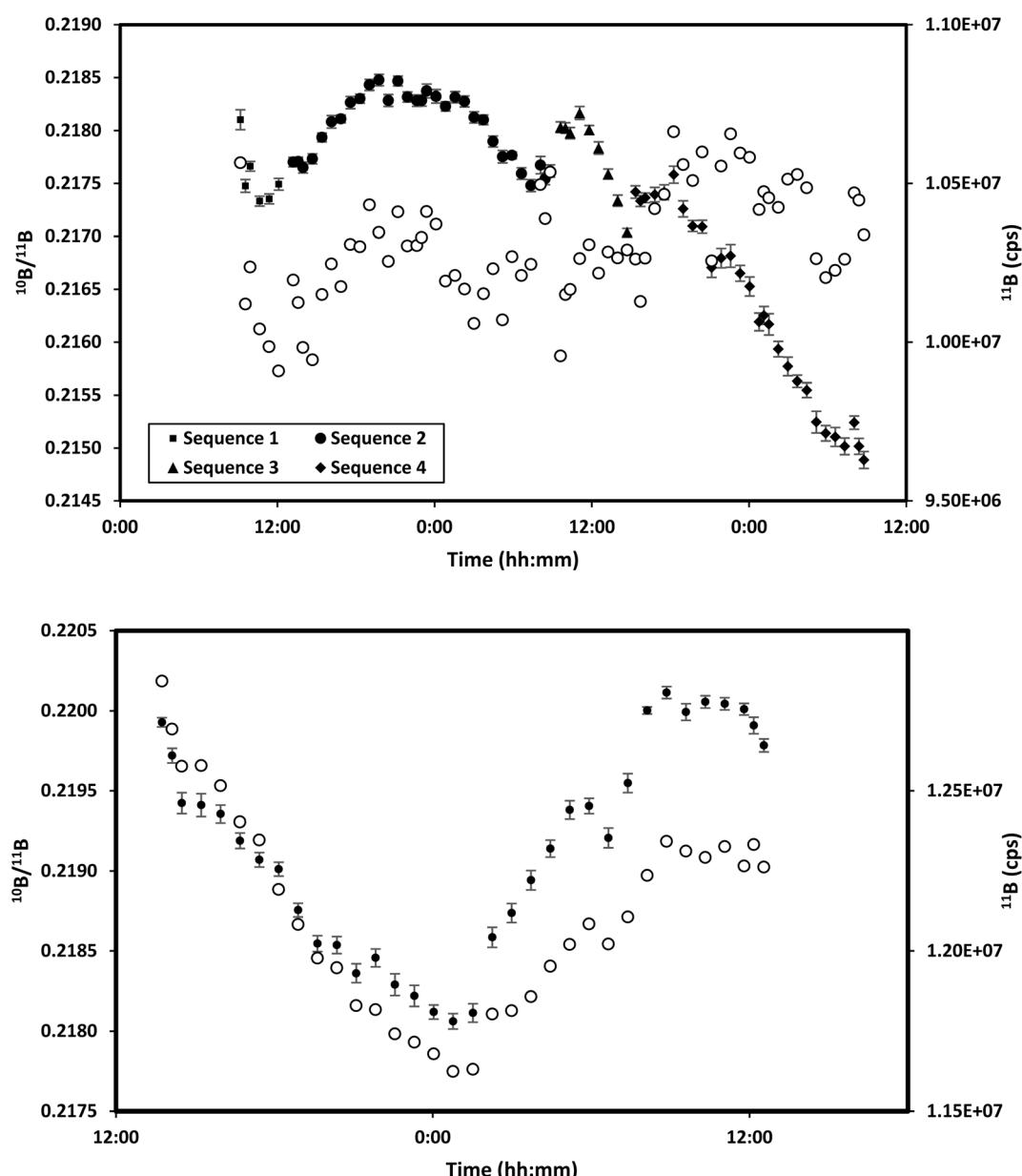
**Fig. 6** Raw $^{10}B/^{11}B$ of the primary standard (GFS Chemicals boric acid) throughout two analytical sessions (A and B, respectively). The white circles correspond to the ^{11}B beam intensity. The plasma was ignited ~2 hours before the beginning of sequence 1 and ~22 hours before the beginning of the sequence in session 2 and remained on throughout the duration of the sessions. Each session corresponds to a distinct period of time in which the plasma was on continuously.

This journal is © The Royal Society of Chemistry 2026

J. Anal. At. Spectrom., 2026, **41**, 513–525 | **521**

sessions from which data were produced for this study. Fig. 6a shows the first continuous multi-day session (∼48 hours) in which boron isotopes were measured on the instrument. One observation is that the change in raw boron isotopic composition of the primary standard (GFS Chemicals boric acid) is not correlated with changes in sensitivity over the same period (Fig. 6a). In contrast, the raw boron isotopic composition deviated systematically with changes in sensitivity during the second session (Fig. 6b). Similar figures for the third and fourth analytical sessions from this study are provided in the supplementary file. During the first session, the total variation in the isotopic composition (16‰) is much greater than the average internal precision of individual measurements (0.28‰, 2SE). This drift in raw isotopic ratios reflects changes in the conditions of mass bias through time that are corrected using the sample–standard bracketing technique. During the first session, the primary standard was measured relative to itself a total of eight times with an external precision of 1.36‰ (2SD). During sessions 2, 3, and 4, a secondary boron ICP standard from Inorganic Ventures was measured and gave an external precisions of 1.28‰, 0.31‰, and 3.26‰ (2SD). This demonstrates both the effectiveness and the necessity for sample–standard bracketing techniques for isotope ratio analysis by MC-ICP-MS. However, differences in the external reproducibility between sessions show that factors associated with instrument error likely contribute to the overall uncertainty of B isotopic measurements.

Fig. 7 shows an example of how the double Wien filter tuning can impact the internal precision and as a result the external precision of isotopic ratio measurements. The pre-filter scan feature that scans the electric field while maintaining all other voltages constant shows a "plateau" of isotopic ratio stability across a small voltage range of the E field. During session 4, when the reproducibility of the Inorganic Ventures standard was the poorest, it is likely that the tuning of the double Wien filter was not optimized to produce a stable isotopic ratio. As demonstrated in Fig. 7, tuning to maximize sensitivity may not be adequate for obtaining isotopic ratio data. Only a 10 V difference in a single lens setting of the MS/MS can lead to poor isotopic ratio stability, as illustrated by the lack of a flat peak in Fig. 7b.

4.2 Use of the boric acid standard for isotopic composition measurements

Literature $^{10}B/^{11}B$ values of seawater using various analytical methods range from 0.2383 (ref. 33) to 0.2377.[34] The seawater value measured here is consistent with these values and the more precise value measured in ref. 31 (Table 5). Although the GFS Chemicals boric acid is not certified for isotopic composition, $^{10}B/^{11}B$ values normalized to this standard, assuming an equivalent isotopic composition to NIST951, are within the range of published values for the materials presented here. Alternatively, $^{10}B/^{11}B$ can be renormalized to seawater assuming the value reported in ref. 31, which would decrease the $^{10}B/^{11}B$ by 0.0002 to 0.0006; not a significant deviation relative to the expanded uncertainties of the measurements. The data presented here indicate that the GFS Chemicals boric acid solution used as the primary standard has $^{10}B/^{11}B$ within 0.8‰ of the NIST951 boric acid certified isotopic standard.
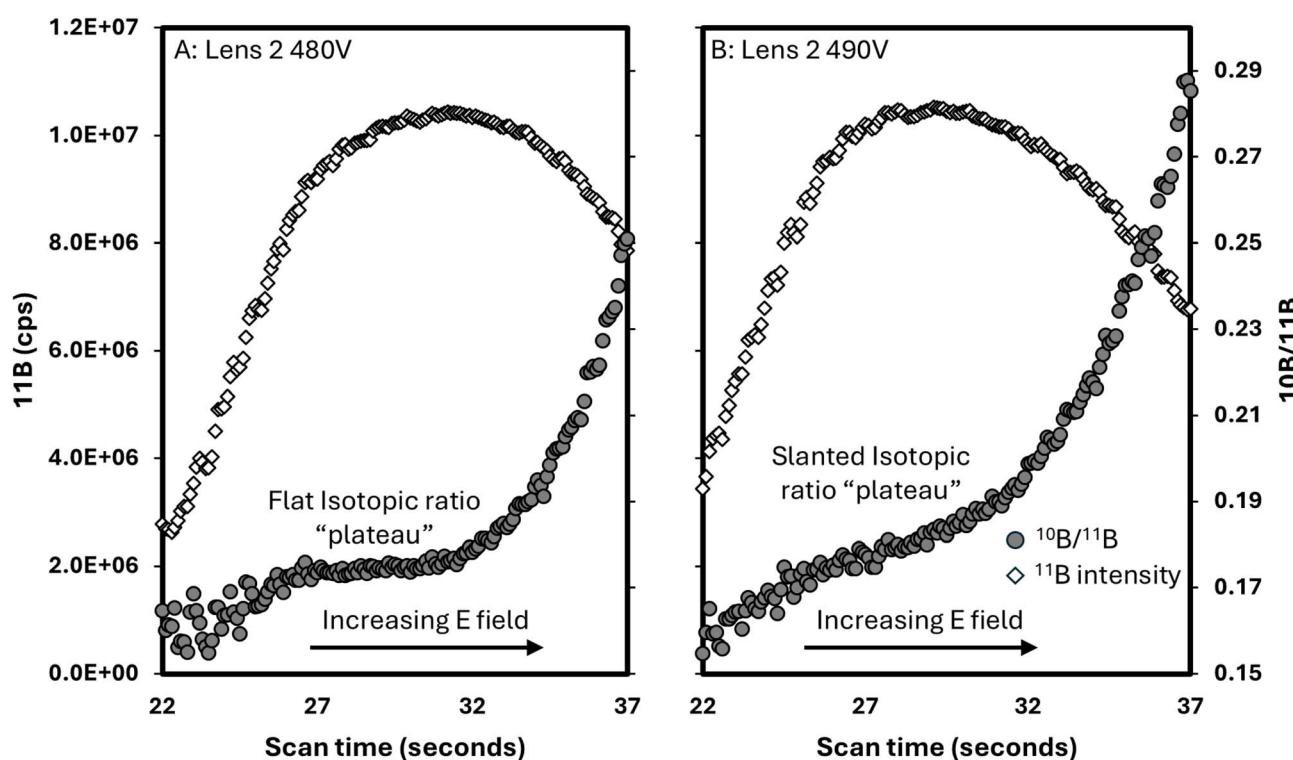

Fig. 7 Pre-filter electric (E) field scans at lens 2 settings of 480 V (A) and 490 V (B) of the MS/MS.

522 | J. Anal. At. Spectrom., 2026, 41, 513–525

This journal is © The Royal Society of Chemistry 2026

4.3 Impact of low recoveries on isotopic composition

Low recovery of boron can result from volatilization during the evaporation process, not collecting the full elution peak during the boron chemical separations, or an incomplete digestion process, all of which would lead to isotopic fractionation of boron in the final sample relative to the true value. One aspect of the chemistry procedure used in this study that we found problematic was the dry-down of the sample after the first column. Once the sample was dried completely, the residue became static-sensitive and small pieces of the residue were observed to exit the PFA vial when the sample was pulled from the hotplate at the moment of dryness. Precautions to avoid sample loss included placing the cap of the vial on the beaker before removing it from the hotplate. If the sample residue during this stage of the process had a homogenous boron isotopic composition, then loss of boron during this step would result in low recoveries but would not lead to isotopic fractionation of the final sample aliquot. Given the relatively low recoveries, but accurate isotopic compositions of some samples, loss of boric due to static removal of sample residue is a possible scenario.

4.4 Impact of blanks on isotopic composition

Elevated B blanks resulting from the digestion and purification procedures impact materials with low B concentrations. The $^{10}B/^{11}B$ of the session 1 blank was nearly identical to the values measured for W-2a (0.2449 in the blank $vs.$ 0.2444 in W-2a). It is possible that the high blank was the result of cross contamination with W-2a, due either to undetected volatility of boron or to contamination from the dry-down after the first column procedure that resulted in static-sensitive residues. Good agreement between literature and blank-corrected measured values for all materials indicates that a blank correction is indeed necessary for all measurements. The magnitude of the correction is largest for materials with the lowest B concentrations, such as BIR-1a, BHVO-2, and T1-G (Table 5). This highlights the care that is required to maintain low blanks during boron separation procedures and analysis, especially for samples with low boron contents.

4.5 Recommendations for B isotopic compositions

Despite efforts by this study and the scientific community to minimize blanks, volatilization, and other sources of fractionation and inaccuracies, considerable scatter persists in B isotope composition of reference materials in the literature

($e.g.$, Fig. 5). Regardless of B concentration and methods for sample processing and analysis by mass spectrometry, inter-laboratory reproducibility of silicate reference materials is limited to ~1.7‰ for the $\delta^{11}B$ value. For example, IAEA B-6 has reported measurements by MC-ICP-MS,[18,22,23,35–38] positive (P)-TIMS,[36,39] LA-MC-ICP-MS,[9,35,40] and Neoma MS/MS MC-ICP-MS (this study) with obvious improvement in measurement precision between different methods (Fig. 5). This suggests that the scatter observed between different laboratory measurements is likely due to the challenges in dissolution without loss or fractionation of B rather than the analytical measurement strategy. Table 6 comprises values for reference materials with multiple measurements in the literature that were also measured in this study, which we propose as recommended values for these materials, including IAEA B-6, and USGS rock reference materials BCR-2, BHVO-2, BIR-1, and W-2. As mentioned previously, BIR-1 contains very low B concentrations and therefore has the highest uncertainty in B isotopic composition. However, W-2a, with a much higher concentration of B, shows similar variability in isotopic composition as BIR-1a. The origins of this variation are therefore not solely attributed to low boron/blank contributions, and sample heterogeneity cannot be ruled out. These values can be used as general guidelines for B isotope ratio quality control, albeit with relatively low precision.

5. Conclusions

In this work we developed a method for B isotope analysis of bulk silicate materials using an HF digestion/extraction followed by a two-step ion exchange procedure. The method is also applicable to analyses of seawater. We present an evaluation of the use of the Neoma MS/MS MC-ICP-MS for analyses of B isotopes in solutions. $^{10}B/^{11}B$ results for seawater and IAEA B-6, BCR-2, BHVO-2, and W-2a reference materials agree with literature values. $^{10}B/^{11}B$ results for BIR-1a are close to values measured in BIR-1G after blank correction, while the value measured in AGV-2 is distinct from that measured in AGV-2G in this study. The performance of the Neoma over multiple sessions shows that drift in isotopic composition of the primary standard can be corrected using sample–standard bracketing techniques, consistent with previous generation instruments. While the precision of $^{10}B/^{11}B$ isotopic measurements is constrained by the $^{10}B/^{11}B$ uncertainty of the reference standard (0.08% or 0.8‰), additional uncertainties associated with potential volatilization, incomplete yields, and blank contributions during sample processing seem to limit the overall uncertainty to at least 1.7‰ based on interlaboratory reproducibility. Heterogeneity of samples also cannot be ruled out.

Conflicts of interest

There are no conflicts of interest to declare.

Data availability

The data supporting this article are included in the manuscript.

Table 6 Recommended $\delta^{11}B$ values for reference materials

Reference material	$\delta^{11}B$ (‰)	2SD	n
IAEA B-6	−2.57	1.97	16
USGS BCR-2	−5.57	1.67	7
USGS BHVO-2	−2.19	2.47	8
USGS BIR-1(a)	−2.69	4.87	3
USGS W-2(a)	9.79	4.90	6

This journal is © The Royal Society of Chemistry 2026

$J. Anal. At. Spectrom.$, 2026, **41**, 513–525 | **523**

Acknowledgements

References

1 H. G. Thode, J. Macnamara, F. P. Lossing and C. B. Collins, Natural Variations in the Isotopic Content of Boron and its Chemical Atomic Weight, *J. Am. Chem. Soc.*, 1948, **70**(9), 3008–3011.

2 J. Xiao, Y. K. Xiao, Z. D. Jin, M. Y. He and C. Q. Liu, Boron isotope variations and its geochemical application in nature, *Aust. J. Earth Sci.*, 2013, **60**(4), 431–447.

3 Advances in Isotope Geochemistry, *Boron Isotopes*, ed. H. Marschall and G. Foster, Springer International Publishing, Cham, 2018, DOI: 10.1007/978-3-319-64666-4.

4 S. Barth, Boron isotope variations in nature: a synthesis, *Geol. Rundsch.*, 1993, **82**(4), DOI: 10.1007/BF00191491.

5 C. Subramanian, A. K. Suri and T. S. R. C. Murthy, Development of Boron-based materials for nuclear applications, *BARC Newsl.*, 2010, **313**, 14–22.

6 S. A. R. Wynchank, A. E. Cox and C. H. Collie, The thermal neutron capture cross section of a natural boron, *Nucl. Phys.*, 1965, **62**(3), 491–496.

7 C. Kurta, L. Dorta, F. Mittermayr, K. Prattes, B. Hattendorf, D. Günther, *et al.*, Rapid screening of boron isotope ratios in nuclear shielding materials by LA-ICPMS – a comparison of two different instrumental setups, *J. Anal. At. Spectrom.*, 2014, **29**(1), 185–192.

8 G. L. Foster, B. Hönisch, G. Paris, G. S. Dwyer, J. W. B. Rae, T. Elliott, *et al.*, Interlaboratory comparison of boron isotope analyses of boric acid, seawater and marine CaCO3 by MC-ICPMS and NTIMS, *Chem. Geol.*, 2013, **358**, 1–14.

9 K. Hou, Y. Li, Y. Xiao, F. Liu and Y. Tian, In situ boron isotope measurements of natural geological materials by LA-MC-ICP-MS, *Chin. Sci. Bull.*, 2010, **55**(29), 3305–3311.

10 H. R. Marschall and B. D. Monteleone, Boron Isotope Analysis of Silicate Glass with Very Low Boron Concentrations by Secondary Ion Mass Spectrometry, *Geostand. Geoanal. Res.*, 2015, **39**(1), 31–46.

11 N. E. Sievers, C. A. Menold, M. Grove and M. A. Coble, White mica trace element and boron isotope evidence for distinctive infiltration events during exhumation of deeply subducted continental crust, *Int. Geol. Rev.*, 2017, **59**(5–6), 621–638.

12 C. D. Standish, J. A. Milton, R. M. Brown and G. L. Foster, Matrix independent and interference free *in situ* boron isotope analysis by laser ablation MC-ICP-MS/MS, *J. Anal. At. Spectrom.*, 2025, **40**, 1309–1322.

13 E. J. Catanzaro, C. E. Champion, E. L. Garner, G. Marinenko, K. M. Sappenfield and W. R. Shields, *Standard Reference Materials : Boric Acid; Isotopic, and Assay Standard Reference Materials*, National Institute of Standards and Technology, Washington, DC, 1970, p. 70, Report No.: 260-17.

14 M. Gutjahr, L. Bordier, E. Douville, J. Farmer, G. L. Foster, E. C. Hathorne, *et al.*, Sub-Permil Interlaboratory Consistency for Solution-Based Boron Isotope Analyses on Marine Carbonates, *Geostand. Geoanal. Res.*, 2021, **45**(1), 59–75.

15 K. Kubota, T. Ishikawa, K. Nagaishi, T. Kawai, T. Sagawa, M. Ikehara, *et al.*, Comprehensive analysis of laboratory boron contamination for boron isotope analyses of small carbonate samples, *Chem. Geol.*, 2021, **576**, 120280.

16 M. Trudgill, S. Nuber, H. E. Block, J. Crumpton-Banks, H. Jurikova, E. Littley, *et al.*, A Simple, Low-Blank Batch Purification Method for High-Precision Boron Isotope Analysis, *Geochem., Geophys., Geosyst.*, 2024, **25**(3), e2023GC011350.

17 C. Xu, H. Jurikova, S. Nuber, R. C. J. Steele, M. Trudgill, S. Barker, *et al.*, A Rapid, Simple, and Low-Blank Pumped Ion-Exchange Column Chromatography Technique for Boron Purification From Carbonate and Seawater Matrices, *Geochem., Geophys., Geosyst.*, 2024, **25**(2), e2023GC011228.

18 A. N. Paul, J. A. Stewart, S. Agostini, L. A. Kirstein, J. C. M. De Hoog, I. P. Savov, *et al.*, Refining Boron Isotopic Measurements of Silicate Samples by Multi-Collector-Inductively Coupled Plasma-Mass Spectrometry (MC-ICP-MS), *Geostand. Geoanal. Res.*, 2024, **48**(1), 91–108.

19 T. Ishikawa and E. Nakamura, Suppression of boron volatilization from a hydrofluoric acid solution using a boron-mannitol complex, *Anal. Chem.*, 1990, **62**(23), 2612–2616.

20 E. Nakamura, T. Ishikawa, J. L. Birck and C. J. Allègre, Precise boron isotopic analysis of natural rock samples using a boron-mannitol complex, *Chem. Geol.*, 1992, **94**, 193–204.

21 A. Makishima, E. Nakamura and T. Nakano, Determination of Boron in Silicate Samples by Direct Aspiration of Sample HF Solutions into ICPMS, *Anal. Chem.*, 1997, **69**(18), 3754–3759.

22 G. J. Wei, J. Wei, Y. Liu, T. Ke, Z. Ren, J. Ma, *et al.*, Measurement on high-precision boron isotope of silicate materials by a single column purification method and MC-ICP-MS, *J. Anal. At. Spectrom.*, 2013, **28**(4), 606–612.

23 X. Li, H. Y. Li, J. G. Ryan, G. J. Wei, L. Zhang, N. B. Li, *et al.*, High-precision measurement of B isotopes on low-boron oceanic volcanic rock samples via MC-ICPMS: Evaluating acid leaching effects on boron isotope compositions, and B isotopic variability in depleted oceanic basalts, *Chem. Geol.*, 2019, **505**, 76–85.

24 J. lien Pi, C. F. You and C. H. Chung, Micro-sublimation separation of boron in rock samples for isotopic measurement by MC-ICPMS, *J. Anal. At. Spectrom.*, 2014, **29**(5), 861–867.

25 S. Tonarini, M. Pennisi and W. P. Leeman, Precise boron isotopic analysis of complex silicate (rock) samples using alkali carbonate fusion and ion-exchange separation, *Chem. Geol.*, 1997, **142**(1–2), 129–137.

26 J. Gaillardet, D. Lemarchand, C. Göpel and G. Manhès, Evaporation and Sublimation of Boric Acid: Application for Boron Purification from Organic Rich Solutions, *Geostand. Newsl.*, 2001, **25**(1), 67–75.

27 E. Kiss, Ion-exchange separation and spectrophotometric determination of boron in geological materials, *Anal. Chim. Acta*, 1988, **211**, 243–256.

28 G. Craig, H. Wehrs, D. G. Bevan, M. Pfeifer, J. Lewis, C. D. Coath, *et al.*, Project Vienna: A Novel Precell Mass Filter for Collision/Reaction Cell MC-ICPMS/MS, *Anal. Chem.*, 2021, **93**(30), 10519–10527.

29 N. S. Lloyd, S. A. Yu and S. Misra, Application of 10^{13} ohm Faraday cup current amplifiers for boron isotopic analyses by solution mode and laser ablation multicollector inductively coupled plasma mass spectrometry, *Rapid Commun. Mass Spectrom.*, 2018, **32**(1), 9–18.

30 K. P. Jochum, U. Weis, B. Schwager, B. Stoll, S. A. Wilson, G. H. Haug, *et al.*, Reference Values Following ISO Guidelines for Frequently Requested Rock Reference Materials, *Geostand. Geoanal. Res.*, 2016, **40**(3), 333–350.

31 G. L. Foster, P. A. E. Pogge Von Strandmann and J. W. B. Rae, Boron and magnesium isotopic composition of seawater, *Geochem., Geophys., Geosyst.*, 2010, **11**(8), 2010GC003201.

32 M. He, X. Xia, X. Huang, J. Ma, J. Zou, Q. Yang, *et al.*, Rapid determination of the original boron isotopic composition from altered basaltic glass by *in situ* secondary ion mass spectrometry, *J. Anal. At. Spectrom.*, 2020, **35**(2), 238–245.

33 A. Vengosh, Y. Kolodny, A. Starinsky, A. R. Chivas and M. T. McCulloch, Coprecipitation and isotopic fractionation of boron in modern biogenic carbonates, *Geochim. Cosmochim. Acta*, 1991, **55**(10), 2901–2910.

34 J. Gaillardet and C. J. Allègre, Boron isotopic compositions of corals: Seawawter or diagenesis record?, *Earth Planet. Sci. Lett.*, 1995, **136**, 665–676.

35 R. Gonfiantini, S. Tonarini, M. Gröning, A. Adorni-Braccesi, A. S. Al-Ammar, M. Astner, *et al.*, Intercomparison of Boron Isotope and Concentration Measurements. Part II: Evaluation of Results, *Geostand. Newsl.*, 2003, **27**(1), 41–57.

36 V. Devulder, P. Degryse and F. Vanhaecke, Development of a Novel Method for Unraveling the Origin of Natron Flux Used in Roman Glass Production Based on B Isotopic Analysis via Multicollector Inductively Coupled Plasma Mass Spectrometry, *Anal. Chem.*, 2013, **85**(24), 12077–12084.

37 G. Zhu, J. Ma, G. Wei and L. Zhang, Boron Mass Fractions and δ^{11} B Values of Eighteen International Geological Reference Materials, *Geostand. Geoanal. Res.*, 2021, **45**(3), 583–598.

38 Y. Cai, E. T. Rasbury, K. M. Wooton, X. Jiang and D. Wang, Rapid boron isotope and concentration measurements of silicate geological reference materials dissolved through sodium peroxide sintering, *J. Anal. At. Spectrom.*, 2021, **36**(10), 2153–2163.

39 S. Tonarini, M. Pennisi, A. Adorni-Braccesi, A. Dini, G. Ferrara, R. Gonfiantini, *et al.*, Intercomparison of Boron Isotope and Concentration Measurements. Part I: Selection, Preparation and Homogeneity Tests of the Intercomparison Materials, *Geostand. Newsl.*, 2003, **27**(1), 21–39.

40 R. O. C. Fonseca, M. Kirchenbaur, C. Ballhaus, C. Münker, A. Zirner, A. Gerdes, *et al.*, Fingerprinting fluid sources in Troodos ophiolite complex orbicular glasses using high spatial resolution isotope and trace element geochemistry, *Geochim. Cosmochim. Acta*, 2017, **200**, 145–166.

41 J. D. Xu, A. Gerdes, A. Schmidt, D. C. Hezel and H. R. Marschall, Simultaneous Bulk-Rock Elemental and Boron Isotope Ratio Measurement Using LA - ICP - MS on Silicate Micro-Particulate Pellets, *Geostand. Geoanal. Res.*, 2024, **48**(4), 807–822.

42 J. Zhang, Z. Bai, H. Zheng, C. Zhao, Y. Ding, Z. Lu, *et al.*, Characterizing the shaping, transmission, and amplification of near flat-top Gaussian beams through soft-edged apertures, *Opt. Express*, 2024, **32**(22), 39293.

43 Y. H. Liu, K. F. Huang and D. C. Lee, Precise and accurate boron and lithium isotopic determinations for small sample-size geological materials by MC-ICP-MS, *J. Anal. At. Spectrom.*, 2018, **33**(5), 846–855.

44 D. Evans, A. Gerdes, D. Coenen, H. R. Marschall and W. Müller, Accurate correction for the matrix interference on laser ablation MC-ICPMS boron isotope measurements in $CaCO_3$ and silicate matrices, *J. Anal. At. Spectrom.*, 2021, **36**(8), 1607–1617.

45 C. Ercolani, D. Lemarchand and A. Dosseto, Insights on catchment-wide weathering regimes from boron isotopes in riverine material, *Geochim. Cosmochim. Acta*, 2019, **261**, 35–55.

This journal is © The Royal Society of Chemistry 2026

J. Anal. At. Spectrom., 2026, **41**, 513–525 | **525**